Nanoparticle-induced augmentation of neutrophils' phagocytosis of bacteria

Kathryn M. Rubey[1], Alexander R. Mukhitov[2], Jia Nong[2,3], Jichuan Wu[2,3], Vera P. Krymskaya[2], Jacob W. Myerson*[3], G. Scott Worthen*[1], Jacob S. Brenner*[2,3]

[1] Children's Hospital of Philadelphia, Department of Pediatrics, Philadelphia, PA, USA
[2] University of Pennsylvania, Department of Medicine, Philadelphia, PA, USA
[3] University of Pennsylvania, Department of Pharmacology, Philadelphia, PA, USA

*** Correspondence:**
Jacob W. Myerson, myerson@pennmedicine.upenn.edu
G. Scott Worthen, worthen@chop.edu
Jacob S. Brenner, jacob.brenner@pennmedicine.upenn.edu

Keywords: nanoparticle, nanomedicine, neutrophil, phagocytosis, opsonization, complement

Abstract

Despite the power of antibiotics, bacterial infections remain a major killer, due to antibiotic resistance and hosts with dysregulated immune systems. We and others have been developing drug-loaded nanoparticles that home to the sites of infection and inflammation via engineered tropism for neutrophils, the first-responder leukocytes in bacterial infections. Here, we examined how a member of a broad class of neutrophil-tropic nanoparticles affects neutrophil behavior, specifically questioning whether the nanoparticles attenuate an important function, bacterial phagocytosis. We found these nanoparticles actually *augment* phagocytosis of non-opsonized bacteria, increasing it by ~50%. We showed this augmentation of phagocytosis is likely co-opting an evolved response, as opsonized bacteria also augment phagocytosis of non-opsonized bacteria. Enhancing phagocytosis of non-opsonized bacteria may prove particularly beneficial in two clinical situations: in hypocomplementemic patients (meaning low levels of the main bacterial opsonins, complement proteins, seen in conditions such as neonatal sepsis

and liver failure) or for bacteria that are largely resistant to complement opsonization (e.g., *Neisseria*). Additionally, we observe that; a) prior treatment with bacteria augments neutrophil uptake of neutrophil-tropic nanoparticles; b) neutrophil-tropic nanoparticles colocalize with bacteria inside of neutrophils. The observation that neutrophil-tropic nanoparticles enhance neutrophil phagocytosis and localize with bacteria inside neutrophils suggests that these nanoparticles will serve as useful carriers for drugs to ameliorate bacterial diseases.

1 Introduction

The introduction of antibiotics last century has left the lay public thinking that bacterial infections are a relatively solved problem, but the clinical reality is that these diverse diseases still cause a huge number of deaths and severe illnesses, even when antibiotics are used (*Pneumonia*, no date; File and Marrie, 2010; Xu *et al.*, 2020; Rubey and Brenner, 2021). The reasons for incomplete effectiveness include at least 3 major factors: First, the “host response” to bacteria is often deleterious, epitomized by sepsis-induced organ failure(Pechous, 2017; Lelubre and Vincent, 2018). Second, bacterial resistance to antibiotics is rising precipitously(Boucher *et al.*, 2009; Reardon, 2015; Centers for Disease Control and, 2019). Third, many hosts, by virtue of age, underlying condition, or therapeutic regimen, are immunocompromised and unable to clear bacteria even in the presence of antibiotics(Grant and Hung, 2013; Tosi *et al.*, 2018). All of these problems are compounded by a lack of innovation in therapies compared to other fields(Silver, 2011).

57 To solve this problem, we and others have been developing nanoparticles that
58 can deliver drugs directly to the site of infection (Rubey and Brenner, 2021). This
59 approach may address each of the 3 problems listed above, depending on whether the
60 cargo drug is an antibiotic, whose therapeutic index can be improved by localization, or
61 an immunomodulator. A particularly promising method for targeting these nanoparticles
62 to acute infections is directing the nanoparticles to neutrophils. Neutrophils are "first
63 responder" leukocytes for most acute bacterial infections, and massively accumulate in
64 sites of infection(Yipp *et al.*, 2017). By delivering antibiotics to neutrophils,
65 nanoparticles could improve bacterial killing. This may be especially useful for
66 antibiotics that cannot cross neutrophil membranes, such as aminoglycosides.
67 Alternatively, neutrophil-tropic nanoparticles could deliver anti-inflammatories to
68 modulate some of the neutrophils' more deleterious responses (part of the dysregulated
69 host defense of sepsis (Zemans, Colgan and Downey, 2009)), such as production of
70 tissue damaging mediators such as neutrophil extracellular traps (NETs)(Yipp and
71 Kubes, 2013), reactive oxygen species (ROS), and proteases (Moraes, Zurawska and
72 Downey, 2006). Nanoparticles with tropism for neutrophils have potential to greatly
73 improve most key aspects of acute bacterial infections, and even non-bacterial
74 inflammatory diseases, such as acute respiratory distress syndrome (ARDS), the highly
75 neutrophilic lung inflammation that kills in COVID-19(Sinha *et al.*, 2022).
76 We recently reported a nanomaterials screen to identify nanoparticles with strong
77 tropism to the neutrophils that accumulate in the capillaries of the lungs during
78 inflammation and play a major role in pneumonia, COVID-19, and ARDS(Myerson *et al.*,
79 2022). We found a broad class of nanoparticles with neutrophil-tropism: "nanoparticles

80 with agglutinated proteins" (NAPs). NAPs have surface-accessible proteins arranged in
81 a non-crystalline pattern (meaning agglutinated / amorphous). By contrast, crystalline
82 protein nanoparticles (viral capsids, ferritin, etc), which have their surface proteins
83 arranged in a fixed and regular pattern, do not have neutrophil tropism. We showed this
84 tropism is due to the fact that NAPs rapidly bind the serum proteins, including C3b and
85 other complement proteins, suggesting complement activation, while non-NAPs do not.
86 Complement is an important component of the immune system that aids phagocytic
87 cells in recognizing particulate matter to be phagocytosed. Previous studies have been
88 dedicated to further understanding of complement binding and activation caused by
89 nanoparticles as it can be a barrier to a nanocarrier's therapeutic potential (Scieszka *et*
90 *al.*, 1991; Inturi *et al.*, 2015; Chen *et al.*, 2017; Moghimi and Simberg, 2017; Betker *et*
91 *al.*, 2018; Vu *et al.*, 2019). We have chosen to use this property to our advantage as
92 serum-opsonization of NAPs is essential for their strong neutrophil tropism.
93 To develop NAPs for targeted delivery to neutrophils in infectious diseases, such
94 as pneumonia, we aim here to ensure that NAPs coordinate with the key beneficial
95 functions of neutrophils, and do not negatively impact their function. Previous studies
96 have shown that nanoparticle phagocytosis may decrease neutrophil adhesion and
97 migration(Fromen *et al.*, 2017). Probably the most essential function of neutrophils
98 during infections like pneumonia is phagocytosis of bacteria, since phagocytosis is
99 necessary for killing of certain bacteria(Lee, Harrison and Grinstein, 2003). Here, we
100 tested neutrophil phagocytosis of NAPs before and after neutrophil phagocytosis of the
101 common bacterial pathogen, *E. coli*. We found that NAPs do not negatively impact
102 neutrophil phagocytosis of bacteria and NAPs localize to neutrophils that have also

taken up bacteria. Quite surprisingly, NAPs, given *after* bacteria, enhance efficiency of neutrophils' phagocytosis of bacteria that have not been opsonized by serum proteins. This effect, termed here *second particle augmentation factor (2PAF)* was illustrated in both: flow cytometry and microscopy. Our results suggest applicability of NAPs to two important clinical situations: hypocomplementemic states (e.g., the neonate (Wolach *et al.*, 1994; Kemp and Campbell, 1996; Schelonka and Infante, 1998; McGreal, Hearne and Spiller, 2012; Zimmermann and Jones, 2021) and liver failure) and bacteria that have strong complement-defense mechanisms(Flannagan, Cosío and Grinstein, 2009) (e.g., *Neisseria* coats itself in the complement inhibitor Factor H). In such clinical situations, NAPs' augmentation of bacterial phagocytosis and colocalization with bacteria in neutrophils could provide a major benefit, beyond the benefits of cargo drugs themselves.

2 Results and Discussion

We recently developed a diverse class of nanoparticles with neutrophil-tropism: NAPs(Myerson *et al.*, 2022). In the present study, we focus on a prototypical member of this class, lysozyme-dextran nanogels (hereafter referred to as "nanogels" or NGs). NGs have the benefit for antibiotic delivery of prolonged nanoparticle shelf-life (years at 4C) and a very high drug-to-carrier mass ratio(Myerson *et al.*, 2018, 2019).

In these experiments with nanogels, we again confirmed our previous findings that particle uptake is enhanced by opsonization by complement proteins present in serum(Myerson *et al.*, 2022). When complement protein C3 is depleted from serum via cobra venom factor (CVF)(Haihua *et al.*, 2018), we see a significant decrease in the

127 percent of neutrophils that take up nanogels (Supplemental Figure 1). The green serum
128 nanogels (second green bar) showed ~80% positivity, as compared to the green CVF
129 nanogels (third and fifth green bars) which had ~30% positivity. It has been well
130 established that complement binding to *E. coli* is necessary for neutrophil phagocytosis
131 of the bacteria(Horwitz and Silverstein, 1980; Brekke *et al.*, 2007). We utilized serum-
132 opsonization of both NAPs and *E. coli* bioparticles for these experiments.

133 One of the first tests of whether these nanocarriers can be used to augment
134 bacterial killing is whether neutrophils will take up the nanocarriers after having been
135 exposed to bacteria. In this experiment, diagrammed in Figure 1A, neutrophils were
136 incubated with heat-killed *E. coli* bioparticles which have surface conjugated pHrodo
137 green, a pH-sensitive dye that fluoresces green only when in the low pH environment of
138 the phagosome. After this 60-minute 37°C incubation, the neutrophils were pelleted and
139 washed to remove free bacteria. The neutrophils were then incubated with nanogels for
140 15 minutes, and subjected to flow cytometry. Before exposure to neutrophils, half the
141 samples of *E. coli* were serum-opsonized (hereafter referred to as “Serum EC”), while
142 the other half were not exposed to serum (simply labeled as “EC” in Fig 1). Similarly,
143 nanogels were divided into serum-opsonized (“Serum NG”) and not (simply “NG”).

144 Flow cytometry was gated to analyze neutrophils exclusively (Supplemental
145 Figure 2). Representative flow cytometry dot-plots are depicted in Figure 1B and
146 quantified in n=6 biological replicates in Figure 1D. We compared the summary statistic
147 of the percentage of neutrophils positive for *E. coli* and/or nanogel fluorescence.
148 Among the numerous comparisons that can be made in this dataset, a surprising finding
149 is demonstrated by comparing the first and third *E. coli* uptake values (red bars) in

150 Figure 1D. These conditions measure the fraction of neutrophils that are positive for
151 phagocytosis of *E. coli* that had not been exposed to serum ("EC"). When these
152 neutrophils were incubated with nanogels that had not been exposed to serum (first red
153 bar), 55% of the neutrophils were positive for *E. coli* phagocytosis. This percentage of
154 neutrophils positive for *E. coli* went up to 85% if the nanogels had been pre-opsonized
155 by serum. This means that serum-opsonized nanogels are able to augment *E. coli*
156 phagocytosis. This augmentation occurred even though the nanogels were delivered
157 *after* free *E. coli* had been washed away from the neutrophils.

158 We term this enhancement the "second particle augmentation factor" (2PAF) and
159 define it for this particular experiment (Fig 1) as the following ratio: (% neutrophils
160 positive for EC phagocytosis when the second delivered particle is Serum NG) / (%
161 neutrophils positive for EC phagocytosis when the second delivered particle is [non-
162 serum-exposed] NG). 2PAF can be more generally defined as: (% neutrophils positive
163 for particle #1 phagocytosis, given that particle #2 is serum-opsonized) / (% neutrophils
164 positive for particle #1 phagocytosis, given that particle #2 was not exposed to serum);
165 where particle #1 refers to the particle (or microbe) neutrophils are exposed to in the
166 first incubation, and particle #2 refers to the second incubation. Thus, a 2PAF > 1
167 indicates that serum-opsonized particle #2 are able to augment phagocytosis of particle
168 #1 (as compared to the control condition, which uses particle #2 that was not exposed
169 to serum). Calculating the 2PAF for non-serum exposed *E. coli* (EC), we thus get
170 2PAF = 85% / 55% = 1.55, meaning that serum-opsonized nanogels increase neutrophil
171 phagocytosis of these *E. coli* by 50% (Fig 1D, inset, blue bar). A 2PAF > 1 is only found
172 when the *E. coli* have not been serum opsonized: 2PAF = 1 when using serum-

173 opsonized *E. coli*, a 0% increase (Fig 1D, inset). Thus, serum-opsonized nanogels are
174 able to augment uptake of non-opsonized bacteria, but not opsonized bacteria, the latter
175 of which are already phagocytosed so extensively (~100%) that we cannot detect
176 improvement within the dynamic range of this assay. The mechanism by which serum
177 enhances NAP phagocytosis is through coating the particles with complement proteins
178 (e.g., C3), as shown previously (Myerson *et al.*, 2022), and in Supplementary Figure 1.
179 This suggests that serum-opsonized nanogels would be most effective in augmenting
180 phagocytosis of bacteria that are not complement-opsonized, such as bacteria that
181 evade complement by covering themselves with Factor H (*Neisseria*, etc), or bacterial
182 infections in hypocomplementemic hosts (e.g., neonatal sepsis).

183 A hypothesis to explain this enhancement is outlined in Figure 1C. The
184 neutrophils are first incubated with green *E. coli* that fluoresce only when in the
185 phagosome, since the *E. coli* is conjugated to the pH-sensitive dye pHrodo green. After
186 incubating the *E. coli* with the neutrophils, free *E. coli* are removed by pelleting and
187 thoroughly washing the neutrophils. However, some *E. coli* remain bound to the surface
188 of the neutrophils (depicted in the second neutrophil of Fig 1C), but they will fluoresce
189 minimally in subsequent flow cytometry unless they are internalized into an acidic
190 compartment. Upon addition of serum-opsonized NGs, these surface-bound *E. coli*
191 become phagocytosed as bystanders when the NGs are phagocytosed (third neutrophil
192 of Fig 1C). This leads to the *E. coli* particles accumulating in the low-pH phagosome,
193 where they fluoresce during flow cytometry. Thus, the use of *E. coli* that fluoresce only
194 in the phagosome allowed detection of a 2PAF > 1.

195 Having made the finding that nanogels can augment phagocytosis of bacteria,
196 we tested whether this was a phenomenon unique to NGs. We performed experiments
197 with NGs replaced as a "second particle" by a second *E. coli* particle, checking whether
198 the second bacterial particles could enhance uptake of bacteria that were delivered
199 during a first incubation. The experimental protocol was the same as Figure 1A, except
200 that particle #1 was pHrodo green *E. coli*, and particle #2 was pHrodo red *E. coli* (Fig
201 2A). Here, the relevant conditions to compare are Figure 2C's first vs. third green bars.
202 This shows that phagocytosis of EC (non-serum exposed *E. coli*) is augmented by
203 subsequent delivery of Serum EC (serum-opsonized *E. coli*). Indeed, the 2PAF = 1.65,
204 or a 65% increase, (Fig 2C, inset, blue bar) is very similar to the 2PAF = 1.55 achieved
205 with nanogels as particle # 2 (Fig 1C, inset, blue bar). Once again, the 2PAF is > 1 only
206 when the first-delivered particle (EC) had not been opsonized. Thus, the NGs' ability to
207 augment uptake of bacteria is not unique to NGs, but is recapitulated in the neutrophil
208 response to bacterial pathogens given in sequence. Our prior work shows that NGs, like
209 bacteria, have tropism for neutrophils due to their rapid opsonization by complement
210 (Myerson *et al.*, 2022). The parallel 2PAF effects for NGs and *E. coli* coincide with these
211 similar uptake mechanisms.
212 Having established that both serum-opsonized NGs and serum-opsonized
213 bacteria can augment phagocytosis of non-opsonized bacteria, we questioned whether
214 NG uptake could be similarly enhanced. We used the same protocol as above, except
215 with particle #1 as NGs (green), and particle #2 as a separate sample of NGs (red) (Fig
216 3A). Comparing the first and third green bars in Fig 3C, we see that serum-opsonized
217 NGs are *minimally* able to augment phagocytosis of *previously* delivered NGs. Thus,

218 2PAF = 1.23. These results may be attributed to difference in fluorophores of the *E. coli*
219 bioparticles and NGs, as NGs fluoresce equally well on the surface of neutrophils (pH 7)
220 and in phagosomes (pH 4-5). More likely though, the low levels of first incubation NG
221 fluorescence observed in the first and third green bars suggest that neutrophils do not
222 retain nanogels on their surface after washing, which would thus prevent augmentation
223 by nanogels delivered during the second incubation. Figure 3C also shows that non-
224 opsonized particle #2 NG uptake (the first red bar) is higher than non-opsonized particle
225 #1 NG uptake (the first green bar). This implies that exposure of neutrophils to a first
226 particle (even one that is mostly washed away) increases the phagocytic efficiency of
227 the neutrophils for nanoparticles that are delivered later. This finding is consistent with
228 previous studies showing neutrophils are known to change their activity state after
229 phagocytosis(Bazzoni *et al.*, 1991). This finding suggests that the order and timing of
230 particle delivery matter significantly.

231 Finally, we administered *E. coli* as particle #2 after NGs as particle #1 (Figure
232 4A). As in Figure 3, when NGs are delivered first, their uptake is minimally augmented
233 by a second particle with 2PAF = 1.17, even when the second particle is highly
234 stimulatory serum-opsonized *E. coli* (Fig 4C, first vs third green bars).

235 Figure 4 also shows that delivery of NGs *before E. coli* does not impair
236 neutrophils' uptake of *E. coli*: levels of *E. coli* uptake were identical for all conditions
237 tested in Fig 4C. This is an important result in the path to clinical translation of
238 neutrophil-tropic nanoparticles, as such nanoparticles might compromise therapy if they
239 inhibited subsequent phagocytosis of bacteria.

240 Taken together, the data presented here strongly indicate that serum-opsonized
241 nanogels and *E. coli* augment phagocytosis of non-opsonized bacteria. We sought to
242 confirm and extend these flow cytometry results with a complementary approach.
243 Therefore, we performed a similar protocol of exposing neutrophils to nanogels and
244 bacteria, but this time we analyzed the cells using microscopy. Not only could this
245 serve as a confirmation of the flow cytometry results, but imaging data additionally can
246 determine if the particles #1 and #2 co-localize with each other within the cell, which
247 gives further insight into the 2PAF phenomenon.

248 We began this line of experiments by performing the same sequential delivery
249 protocol used in flow cytometry experiments, but instead of flow cytometry, cells were
250 fixed in suspension with paraformaldehyde and adhered to glass for microscopy
251 imaging. Figures 5 A-C provide representative microscopy data. Fig 5A shows data
252 where both particle #1 and particle #2 are *E. coli*. We found the same result as in flow
253 cytometry: Serum EC delivered as particle #2 augmented neutrophil phagocytosis of
254 (non-opsonized) EC delivered as particle #1 (compare green & yellow signals in Figs
255 5Aii vs 5Ai). Yellow signal in Fig 5A indicates intracellular overlap between green
256 (particle #1) and red (particle #2) *E. coli* inside of neutrophils, consistent with a large
257 fraction of particle #1 being phagocytosed at the same time and into the same
258 compartment as particle #2. Figure 5B shows data where particle #1 is NGs (green) and
259 particle #2 is *E. coli* (red). In this data, we observe minimal colocalization between the
260 two particles, consistent with flow cytometry data in Figure 4 showing no 2PAF effect
261 when NGs are given before *E. coli*. Figure 5C shows data where particle #1 is *E. coli*
262 (green) and particle #2 is NGs (red). The condition for which flow cytometry yielded

263 2PAF = 1.55 (EC - Serum NG; [Fig 5Cii]), yielded imaging data with a high degree of
264 intracellular overlap between *E. coli* (particle #1) and NGs (particle #2). These imaging
265 data qualitatively support a key conclusion from our quantitative flow cytometry data:
266 opsonized NGs or *E. coli* not only augment uptake of previously delivered, non-
267 opsonized bacteria, but also show localization into similar intracellular compartments.
268 To quantify the data from these microscopy experiments, images of each particle
269 were thresholded via Renyi entropic filtering to identify the portions of each image that
270 were positive for either particle #1 or particle #2. Guided by DiO membrane staining,
271 we identified regions of interest encompassing each cell in each obtained
272 image. Overlaying the thresholded images on the regions of interest corresponding to
273 individual cells allowed us to determine the fraction of pixels in each cell that contained
274 either particle #1 or particle #2. In panels 5D, 5F, and 5H, each point in the presented
275 scatter plots represents the results of this analysis for one neutrophil. The y-axis value
276 for each point represents the percentage of pixels in the neutrophil containing particle
277 #2 and the x-axis value represents the percentage of pixels in the neutrophil containing
278 particle #1. A line was fitted to the data for each condition. Lines with slope = 1 indicate
279 that each neutrophil took up equal quantities of particle #1 and particle #2. Lines with
280 slope > 1 indicate a tendency to take up more of particle #2 than particle #1. Lines with
281 slope < 1 indicate a tendency to take up more of particle #1 than particle #2. We
282 therefore used percentage of positive pixels as a metric for levels of particle #1 and
283 particle #2 uptake in each neutrophil. To derive 2PAF values from the imaging data, we
284 subtracted from our uptake values for each cell the average uptake values for the 2PAF
285 baseline conditions (conditions where particle #2 is not opsonized). We therefore

286 determined our 2PAF value in imaging experiments as the percent *increase* in either
287 particle #1 or particle #2 uptake for each imaged cell vs. the expected level of uptake
288 when particle #2 is not opsonized. These findings are depicted in panels 5E, 5G, and
289 5I.

290 Panels 5D and 5E depict quantitative analysis of imaging data where particles #1
291 and #2 were both *E. coli*. All serum treatment conditions in these experiments showed
292 strong positive correlation between signal from particles #1 and #2, indicating that cells
293 taking up green *E. coli*, given first, were very likely to take up red *E. coli*, delivered
294 second. This confirms this assay behaves as expected: cells do not saturate their *E.*
295 *coli* uptake in this dosing regimen; cells with more uptake of one *E. coli* have more
296 uptake of the second; green and red fluorophores perform equally. As with flow
297 cytometry data in Figure 2C, data in Figure 5E show a clear 2PAF effect exerted by
298 particle #2 *E. coli* on particle #1 *E. coli*. When particle #1 *E. coli* is not opsonized,
299 uptake of particle #1 increases by ~20% if particle #2 *E. coli* is opsonized, compared to
300 data where particle #2 *E. coli* is not opsonized.

301 Panels 5F and 5G depict analysis of imaging data where particle #1 is NGs and
302 particle #2 is *E. coli*. R-squared values were less than 0.1 for all lines in panel 5F
303 except that for Serum+NGs – Serum+*E. coli*, indicating poor linear correlation between
304 particle #1 and particle #2 uptake for the conditions in this data. This indicates that,
305 when a given neutrophil takes up NGs as particle #1, improved uptake of *E. coli* as
306 particle #2 cannot be predicted for that same cell. Similarly, analysis of imaging-based
307 2PAF also indicates no 2PAF effect exerted by particle #2 *E. coli* on particle #1 NGs.
308 All imaging-based 2PAF calculations showed no change in particle #1 NG uptake

309 induced by opsonized particle #2 *E. coli* vs. 2PAF baseline conditions with non-
310 opsonized particle #2 *E. coli*. These data suggest that co-localization is compromised
311 under these conditions, consistent with our understanding that multiple pathways can
312 lead to phagocytosis, not all necessarily leading to accumulation in the identical
313 intracellular compartment(Sahay, Alakhova and Kabanov, 2010).

314 Finally, panels 5H and 5I depict analysis of imaging data where particle #1 is *E.*
315 *coli* and particle #2 is NGs. As with data in panel 5D, panel 5H shows strong positive
316 correlation between particle #1 *E. coli* uptake and particle #2 NG uptake. For all serum
317 treatment conditions, particle #2 NGs were more likely to be taken up in neutrophils that
318 had already taken up particle #1 *E. coli*. This finding contrasts with the data in panel 5F,
319 where, when NGs are given as particle #1, there was no positive correlation between
320 NG uptake and *E. coli* uptake in any given cell. These findings match with analysis of
321 the double-positive (*E. coli*-positive and NG-positive) cell counts in flow cytometry data
322 in the blue bars in Figures 1C and 4C. Panel 5I shows imaging-based 2PAF values for
323 conditions where *E. coli* is particle #1 and NGs are particle #2. Again, these image
324 analysis findings agree with our flow cytometry data: When non-opsonized *E. coli* is
325 particle #1, we observe a 33% increase in *E. coli* uptake per neutrophil when particle #2
326 NGs are serum-treated vs. when particle #2 NGs are not serum-treated. In imaging
327 data, NGs as particle #2 exert a clear 2PAF effect enhancing uptake of *E. coli* as
328 particle #1.

329 For conditions where we observed 2PAF effects (with *E. coli* as both particles #1
330 and #2 or with *E. coli* as particle #1 and NGs as particle #2), neutrophils were also
331 examined with three-dimensional confocal imaging (Supplementary Figures 4 and 5).

For our confocal imaging analysis, we computed quantities of NGs and *E. coli* in each cell as in Figure 5, but quantities of NGs and *E. coli* reflected fluorescent voxels, rather than pixels. Additionally, we quantified voxels that contained both particle #1 and particle #2, directly assessing three-dimensional colocalization of particles #1 and #2 in the confocal images.

For experiments where both particles #1 and #2 were *E. coli*, ~80% of *E. coli* particle #1 signal was spatially colocalized with *E. coli* particle #2 signal when *E. coli* particle #2 was opsonized (panels B-C, green bars 1 and 3 in panel C). Only ~50% of *E. coli* particle #1 signal was spatially colocalized with *E. coli* particle #2 signal when *E. coli* particle #2 was not opsonized (green bar 2 in Supplementary Figure 4, panel C). This finding fits well with a central part of our hypothesis as to the 2PAF mechanism: When there is a 2PAF effect, delayed phagocytosis of particle #1 is driven by coincident uptake of particle #2. In our confocal data, we find that particle #1 *E. coli* is mostly found colocalized with opsonized particle #2 *E. coli* inside neutrophils. This colocalization is diminished under conditions where 2PAF is diminished, when particle #2 *E. coli* is not opsonized. Under conditions with 2PAF effects, particle #2 colocalization with particle #1 (Supplementary Figure 4, panel A, red bars in panel C) was less than particle #1 colocalization with particle #2 (Supplementary Figure 4, panel A, green bars in panel C). This can be attributed to; a) opsonized particle #2 *E. coli* being phagocytosed independently of particle #1 at a higher frequency than events where particle #1 was phagocytosed independently of particle #2; b) opsonized particle #2 *E. coli* being taken up in neutrophils to a greater degree than particle #1 *E. coli*.

354 Panel D in Supplementary Figure 4 indeed indicates higher average uptake values for
355 *E. coli* particle #2 vs. *E. coli* particle #1, especially in 2PAF-affected conditions.
356 Our prototypical 2PAF conditions, where *E. coli* were particle #1 and NGs were
357 particle #2, were also examined in confocal imaging data. Here particle #1 *E. coli*
358 colocalized with particle #2 NGs at ~50-60% frequency when particle #2 NGs were
359 opsonized (Supplementary Figure 5, panels B-C, green bars 1 and 3 in panel C). In
360 comparison, *E. coli* colocalized with NGs at only ~35% frequency under non-2PAF
361 conditions, where particle #2 NGs were not opsonized (Supplementary Figure 5, panels
362 B-C, green bar 2 in panel C). As with data for 2PAF-affected conditions with double *E.*
363 *coli* treatments, *E. coli*-NG 2PAF-affected conditions featured augmented colocalization
364 of particle #1 (*E. coli*) with particle #2 (NGs), implying phagocytosis of particle #1 *E. coli*
365 and particle #2 NGs in the same subcellular locations in neutrophils. Particle #2 NG
366 colocalization with particle #1 *E. coli* (Supplementary Figure 5, panel A, red bars in
367 panel C) was greater than particle #1 *E. coli* localization with NGs (Supplementary
368 Figure 5, panel B, green bars in panel C). This may reflect generally higher uptake of *E.*
369 *coli* vs. NGs (Supplementary Figure 5, panel D), where *E. coli* likely has a higher
370 chance of being taken up in neutrophils independently of NGs, compared to lower
371 quantities of NG uptake meaning NGs have a lower chance of being taken up
372 independently of *E. coli*. Colocalization of particle #2 NGs with particle #1 *E. coli* bodes
373 well for proposed NG drug delivery to neutrophils designed to help augment neutrophil
374 killing of bacteria: When NGs are given after neutrophils have been exposed to
375 bacteria, the NGs end up in the same places as bacteria inside neutrophils.

This study has several limitations. First, the data presented here are all derived from *in vitro* studies. Neutrophil isolation may modify neutrophil function, thus imposing constraints on interpretation. Of note, however, our previous study suggested a good correlation between *in vitro* and *in vivo* observations of NAP uptake in neutrophils (Myerson *et al.*, 2022). Similarly, the *in vivo* environment may contain neutrophil stimuli not seen *in vitro*. Opsonization with normal mouse serum also may not include all of the opsonins that might be present during an inflammatory process, although we have not detected any significantly different effect using acute phase sera (data not shown). Finally, neutrophils are significantly heterogeneous both within and between donors. Accordingly, use of multiple donors reduces this effect, and flow cytometry permits observation of potential heterogeneity, thus mitigating this concern.

3 Materials and Methods

Lysozyme-Dextran Nanogel Synthesis

Lysozyme-dextran nanogels (LDNGs) were synthesized as previously described(Li *et al.*, 2008; Coll Ferrer *et al.*, 2014; Myerson *et al.*, 2018, 2022). Rhodamine-dextran or FITC-dextran (Sigma) and lysozyme from hen egg white (Sigma) were dissolved in deionized and filtered water at a 1:1 or 2:1 mol:mol ratio. Then pH was adjusted to 7.1 and solution was lyophilized. For Maillard reaction, the lyophilized product was heated for 18 hours at 60°C, with 80% humidity maintained via saturated KBr solution in the heating vessel. Dextran-lysozyme conjugates were dissolved in deionized and filtered water to a concentration of 5 mg/mL. Solutions were stirred at 80°C for 30 minutes.

399 Diameter of LDNGs was evaluated with dynamic light scattering (DLS, Malvern) after
400 heat gelation. Particle suspensions were stored at 4°C.
401
402 **Murine serum**
403 Blood was obtained through the inferior vena cava as previously described(Mei *et al.*,
404 2010; Parasuraman, Raveendran and Kesavan, 2010) from B6 wild type mice and
405 pooled. Blood was allowed to clot for 30 minutes at room temperature, and serum was
406 separated by centrifugation of 1500 rpm x 10 minutes at 4°C. Complement proteins
407 were depleted from serum via Cobra Venom Factor as previously described(Haihua *et*
408 *al.*, 2018).
409
410 **Murine neutrophils**
411 Femurs were harvested from B6 wild type mice, and bone marrow was collected and
412 pooled. Neutrophils were isolated from bone marrow via negative selection (Stemcell
413 EasySep™ Mouse Neutrophil Enrichment Kit cat #19762). Neutrophils were suspended
414 in DMEM media at a concentration of 2×10^6 neutrophils/mL. Isolated neutrophils were
415 95% viable by trypan blue, and 80% pure using Ly6g staining and flow cytometry (See
416 Supplementary Figure 1).
417
418 **Nanogel preparation**
419 FITC-labelled lysozyme-dextran NGs were synthesized as above. Stock NGs were
420 brought to a concentration of 5×10^{11} particles/mL. To serum-treat prior to neutrophil
421 incubation, NGs were incubated in 50% serum in DMEM for 1 h at 37°C.

422

423 ***E. coli* BioParticles**

424 For bacterial particles, both pHrodo™ red and green *E. coli* BioParticles™ conjugates
425 (Invitrogen, Thermo Fisher cat #P35361 and #P35366) were used. BioParticles were
426 brought to a concentration of 2mg/mL in PBS. To serum-treat *E. coli* BioParticles prior
427 to neutrophil incubation, BioParticles were incubated in equal volume serum for 1 h at
428 37°C.

429

430 **Prototypical Experiment**

431 **Sequential particle analysis**

432 Neutrophils were isolated and prepared as above. 500uL of neutrophils were incubated
433 with 20uL of either particle while rotating at 37°C. First particle incubation time was 15
434 minutes for NGs and 1 hour for *E. coli* BioParticles, with exception of the conditions with
435 two color *E. coli* BioParticles. In those conditions the first *E. coli* BioParticles incubation
436 was done at 15 minutes to recapitulate the initial NG incubation. Samples were then
437 washed and pelleted 300g x 6 minutes to remove unbound particles. The neutrophils
438 were then resuspended in 500uL DMEM media. The second particle was then
439 incubated with the neutrophils while rotation at 37°C. Second particle incubation time
440 was 15 minutes for NGs and 1 hour for *E. coli* BioParticles, with exception of the
441 conditions with two color NGs. In those conditions the second NG incubation was
442 incubated for 60 minutes to recapitulate the second exposure *E. coli* incubation.
443 Samples were then washed and pelleted again, then resuspended in FACS buffer. For
444 flow cytometry samples, they were stained with anti-Ly6G antibody prior to analysis. For

445 microscopy samples, they were suspended in solution with 2% paraformaldehyde for 30
446 minutes at room temperature, then pelleted and resuspended at a concentration of
447 1 x 10^6/mL.
448
449 **Sample preparation and Confocal microscopy**
450 90µL of paraformaldehyde fixed cells was incubated with 5 x 10^{-7} M DAPI and 1:100
451 Vybrant™ DiD Cell-Labeling Solution (Invitrogen) at 37C for 20 minutes. Samples were
452 centrifuged at 2000g x 1 minute. They were washed with 1mL PBS and sprun at
453 2000RPM x 3 minutes twice. Finally, they were resuspended in 80µL PBS then
454 dropped on cavity slides (Eisco), covered with coverslips (FisherScientific), and
455 analyzed with Leica TCS SP8 Laser confocal microscope. Visualization of neutrophils
456 was performed with water immersion objective HC PL APO CS2 40x/1.10. Images
457 were obtained in sequential scanning mode using Diode 405, OPSL 488, OPSL 552
458 and Diode 638 lasers. We used scan speed 200 Hz and pixel size 0.223 µm for flat
459 images. Z-stacks were obtained with scan speed 600 Hz, XY pixel size 0.223 µm and
460 voxel size 0.424 µm. Images and Z-stacks were processed with LASX (Leica
461 microsystems). Images and Z-stacks were converted to TIFF images for analysis in
462 ImageJ (FIJI distribution 2.1.0/1.53q). Processing and analysis, including image
463 thresholding, fluorescence colocalization, and per-cell analysis of fluorescence signals,
464 employed custom ImageJ macros, code for which is provided in full in the supplement.
465 For per-cell analyses, regions of interest were drawn manually around each imaged cell,
466 using images of DiD membrane stain to define the edges of individual cells.
467

468 **Animal study protocols**

469 All animal studies were carried out in strict accordance with Guide for the Care and Use
470 of Laboratory Animals as adopted by National Institutes of Health and approved by
471 Children's Hospital of Philadelphia Institutional Animal Care and Use Committee. All
472 animal experiments used male B6 mice, 6–8 weeks old, purchased from Jackson
473 Laboratories. Mice were maintained at 20–25 °C, 50% ± 20% humidity, and on a 12/12 h
474 dark/light cycle with food and water ad libitum.

475

476 **Statistical analysis**

477 Error bars indicate the standard error of the mean throughout. Significance tests are
478 described in captions. Statistical power was determined for statements of statistical
479 significance and tabulated in the supplementary materials.

480

481 **4 Conclusion**

482 The data presented here are consistent with a model of neutrophil phagocytosis in
483 which a non-opsonized bacteria, that is poorly phagocytosed, is nonetheless still
484 available in a compartment (likely the surface plasma membrane) from which it can be
485 subsequently taken up in response to a more phagocytic-stimulatory particle, whether it
486 be an opsonized bacteria or an opsonized nanogel. Similarly, initial exposure to a
487 bacterial-like particle further enhances subsequent uptake of nanogels, even non-
488 opsonized ones. Thus, the nanogel might be used in its opsonized form, even without
489 incorporated drugs, to enhance uptake of poorly-opsonized bacteria. Furthermore,
490 under these circumstances, the bacteria and nanoparticles are found in similar

intracellular compartments, suggesting that delivery to specific compartments of the phagocytosing neutrophil might be possible.

Acknowledgements:

We are grateful for the support by the grants from the National Institutes of Health F32-HL-151026 (KMR), RO1-HL-151467 and RO1-HL-158737 (VPK), R01-HL-157189 (VRM/GSW), K08-HL-138269, R01-HL-153510 and R01-HL-160694 (JSB), and UH3-TR-002198 (GSW), as well as, the Job Research Foundation Grant (VPK).

499 **References**

500 Bazzoni, F. *et al.* (1991) 'Phagocytosing neutrophils produce and release high amounts
501 of the neutrophil-activating peptide 1/interleukin 8', *Journal of Experimental Medicine*,
502 173(3), pp. 771–774. doi: 10.1084/jem.173.3.771.

503 Betker, J. L. *et al.* (2018) 'Nanoparticle uptake by circulating leukocytes: A major barrier
504 to tumor delivery', *Journal of Controlled Release*, 286, pp. 85–93. doi:
505 10.1016/j.jconrel.2018.07.031.

506 Boucher, H. W. *et al.* (2009) 'Bad bugs, no drugs: No ESKAPE! An update from the
507 Infectious Diseases Society of America', *Clinical Infectious Diseases*, 48(1), pp. 1–12.
508 doi: 10.1086/595011.

509 Brekke, O.-L. *et al.* (2007) 'The role of complement C3 opsonization, C5a receptor, and
510 CD14 in *E. coli*-induced up-regulation of granulocyte and monocyte CD11b/CD18
511 (CR3), phagocytosis, and oxidative burst in human whole blood', *J. Leukoc. Biol*, 81, pp.
512 1404–1413. doi: 10.1189/jlb.0806538.

513 Centers for Disease Control and (2019) 'Antibiotic resistance threats in the United
514 States', *U.S Department of Health and Human services*, pp. 1–113. doi:
515 10.15620/cdc:82532.

516 Chen, F. *et al.* (2017) 'Complement proteins bind to nanoparticle protein corona and
517 undergo dynamic exchange in vivo', *Nature Nanotechnology*, 12(4), pp. 387–393. doi:
518 10.1038/nnano.2016.269.

519 Coll Ferrer, M. C. *et al.* (2014) 'ICAM-1 targeted nanogels loaded with dexamethasone
520 alleviate pulmonary inflammation', *PLoS ONE*, 9(7), p. 102329. doi:
521 10.1371/journal.pone.0102329.

522 File, T. M. and Marrie, T. J. (2010) ‘Burden of community-acquired pneumonia in North
523 American adults’, *Postgraduate Medicine*, 122(2), pp. 130–141. doi:
524 10.3810/pgm.2010.03.2130.
525 Flannagan, R. S., Cosío, G. and Grinstein, S. (2009) ‘Antimicrobial mechanisms of
526 phagocytes and bacterial evasion strategies’, *Nature Reviews Microbiology*, pp. 355–
527 366. doi: 10.1038/nrmicro2128.
528 Fromen, C. A. *et al.* (2017) ‘Neutrophil-Particle Interactions in Blood Circulation Drive
529 Particle Clearance and Alter Neutrophil Responses in Acute Inflammation’, *ACS Nano*,
530 11(11), pp. 10797–10807. doi: 10.1021/acsnano.7b03190.
531 Grant, S. S. and Hung, D. T. (2013) ‘Persistent bacterial infections, antibiotic tolerance,
532 and the oxidative stress response’, *Virulence*, pp. 273–283. doi: 10.4161/viru.23987.
533 Haihua, C. *et al.* (2018) ‘Cobra Venom Factor-induced complement depletion protects
534 against lung ischemia reperfusion injury through alleviating blood-air barrier damage’,
535 *Scientific Reports*. Springer US, 8(1), pp. 1–8. doi: 10.1038/s41598-018-28724-z.
536 Horwitz, M. A. and Silverstein, S. C. (1980) ‘Influence of the Escherichia coli capsule on
537 complement fixation and on phagocytosis and killing by human phagocytes’, *Journal of
538 Clinical Investigation*, 65(1), pp. 82–94. doi: 10.1172/JCI109663.
539 Inturi, S. *et al.* (2015) ‘Modulatory Role of Surface Coating of Superparamagnetic Iron
540 Oxide Nanoworms in Complement Opsonization and Leukocyte Uptake HHS Public
541 Access’, *ACS Nano*, 9(11), pp. 10758–10768. doi: 10.1021/acsnano.5b05061.
542 Kemp, A. S. and Campbell, D. E. (1996) ‘The neonatal immune system’, *Seminars in
543 Neonatology*. W.B. Saunders, 1(2), pp. 67–75. doi: 10.1016/S1084-2756(05)80002-8.
544 Lee, W. L., Harrison, R. E. and Grinstein, S. (2003) ‘Phagocytosis by neutrophils’,

Microbes and Infection, pp. 1299–1306. doi: 10.1016/j.micinf.2003.09.014.

Lelubre, C. and Vincent, J. L. (2018) 'Mechanisms and treatment of organ failure in sepsis', *Nature Reviews Nephrology*, pp. 417–427. doi: 10.1038/s41581-018-0005-7.

Li, J. *et al.* (2008) 'Lysozyme - Dextran Core - Shell nanogels prepared via a green process', *Langmuir*. American Chemical Society , 24(7), pp. 3486–3492. doi: 10.1021/LA702785B/SUPPL_FILE/LA702785B-FILE003.PDF.

McGreal, E. P., Hearne, K. and Spiller, O. B. (2012) 'Off to a slow start: Under-development of the complement system in term newborns is more substantial following premature birth', *Immunobiology*, 217(2), pp. 176–186. doi: 10.1016/j.imbio.2011.07.027.

Mei, J. *et al.* (2010) 'CXCL5 Regulates Chemokine Scavenging and Pulmonary Host Defense to Bacterial Infection', *Immunity*. NIH Public Access, 33(1), p. 106. doi: 10.1016/J.IMMUNI.2010.07.009.

Moghimi, S. M. and Simberg, D. (2017) 'Complement activation turnover on surfaces of nanoparticles', *Nano Today*, 15, pp. 8–10. doi: 10.1016/j.nantod.2017.03.001.

Moraes, T. J., Zurawska, J. H. and Downey, G. P. (2006) 'Neutrophil granule contents in the pathogenesis of lung injury', *Current Opinion in Hematology*, 13(1), pp. 21–27. doi: 10.1097/01.moh.0000190113.31027.d5.

Myerson, J. W. *et al.* (2018) 'Flexible Nanoparticles Reach Sterically Obscured Endothelial Targets Inaccessible to Rigid Nanoparticles', *Advanced Materials*, 30(32). doi: 10.1002/adma.201802373.

Myerson, J. W. *et al.* (2019) 'Cross-linker-Modulated Nanogel Flexibility Correlates with Tunable Targeting to a Sterically Impeded Endothelial Marker', *ACS Nano*, 13(10), pp.

568 11409–11421. doi: 10.1021/acsnano.9b04789.

569 Myerson, J. W. *et al.* (2022) 'Supramolecular arrangement of protein in nanoparticle
570 structures predicts nanoparticle tropism for neutrophils in acute lung inflammation',
571 *Nature Nanotechnology*, 17(1), pp. 86–97. doi: 10.1038/s41565-021-00997-y.

572 Parasuraman, S., Raveendran, R. and Kesavan, R. (2010) 'Blood sample collection in
573 small laboratory animals', *Journal of Pharmacology and Pharmacotherapeutics*, 1(2),
574 pp. 87–93. doi: 10.4103/0976-500X.72350.

575 Pechous, R. D. (2017) 'With friends like these: The complex role of neutrophils in the
576 progression of severe pneumonia', *Frontiers in Cellular and Infection Microbiology*.
577 Frontiers Media SA, p. 160. doi: 10.3389/fcimb.2017.00160.

578 *Pneumonia* (no date). Available at: https://www.who.int/news-room/fact-
579 sheets/detail/pneumonia (Accessed: 4 March 2021).

580 Reardon, S. (2015) 'Spread of antibiotic-resistance gene does not spell bacterial
581 apocalypse — yet', *Nature*. Springer Science and Business Media LLC. doi:
582 10.1038/nature.2015.19037.

583 Rubey, K. M. and Brenner, J. S. (2021) 'Nanomedicine to fight infectious disease',
584 *Advanced Drug Delivery Reviews*, 179, p. 113996. doi: 10.1016/j.addr.2021.113996.

585 Sahay, G., Alakhova, D. Y. and Kabanov, A. V (2010) 'Endocytosis of nanomedicines',
586 *Journal of Controlled Release*, pp. 182–195. doi: 10.1016/j.jconrel.2010.01.036.

587 Schelonka, R. L. and Infante, A. J. (1998) 'Neonatal immunology', *Seminars in*
588 *Perinatology*. W.B. Saunders, 22(1), pp. 2–14. doi: 10.1016/S0146-0005(98)80003-7.

589 Scieszka, J. F. *et al.* (1991) 'Role of complements C3 and C5 in the phagocytosis of
590 liposomes by human neutrophils', *Pharmaceutical research*. Pharm Res, 8(1), pp. 65–

591 69. doi: 10.1023/A:1015830306839.

592 Silver, L. L. (2011) ‘Challenges of antibacterial discovery’, *Clinical Microbiology*
593 *Reviews*. American Society for Microbiology Journals, 24(1), pp. 71–109. doi:
594 10.1128/CMR.00030-10.

595 Sinha, S. *et al.* (2022) ‘Dexamethasone modulates immature neutrophils and interferon
596 programming in severe COVID-19’, *Nature Medicine*, 28(1), pp. 201–211. doi:
597 10.1038/s41591-021-01576-3.

598 Tosi, M. *et al.* (2018) ‘Multidrug resistant bacteria in critically ill patients: a step further
599 antibiotic therapy’, *Journal of Emergency and Critical Care Medicine*, 2, pp. 103–103.
600 doi: 10.21037/jeccm.2018.11.08.

601 Vu, V. P. *et al.* (2019) ‘Immunoglobulin deposition on biomolecule corona determines
602 complement opsonization efficiency of preclinical and clinical nanoparticles’, *Nature*
603 *Nanotechnology*, 14(3), pp. 260–268. doi: 10.1038/s41565-018-0344-3.

604 Wolach, B. *et al.* (1994) ‘Some aspects of the humoral immunity and the phagocytic
605 function in newborn infants.’, *Israel journal of medical sciences*, 30(5–6), pp. 331–5.
606 Available at: http://www.ncbi.nlm.nih.gov/pubmed/8034475.

607 Xu, J. *et al.* (2020) ‘Mortality in the United States, 2018’, *NCHS data brief*, (355), pp. 1–
608 8.

609 Yipp, B. G. *et al.* (2017) ‘The lung is a host defense niche for immediate neutrophil-
610 mediated vascular protection’, *Science Immunology*. Sci Immunol, 2(10). doi:
611 10.1126/sciimmunol.aam8929.

612 Yipp, B. G. and Kubes, P. (2013) ‘NETosis: how vital is it?’, *Blood*. American Society of
613 Hematology, 122(16), pp. 2784–2794. doi: 10.1182/BLOOD-2013-04-457671.

614 Zemans, R. L., Colgan, S. P. and Downey, G. P. (2009) 'Transepithelial migration of
615 neutrophils: Mechanisms and implications for acute lung injury', *American Journal of*
616 *Respiratory Cell and Molecular Biology*, pp. 519–535. doi: 10.1165/rcmb.2008-0348TR.
617 Zimmermann, P. and Jones, C. E. (2021) 'Factors That Influence Infant Immunity and
618 Vaccine Responses', *The Pediatric infectious disease journal*. NLM (Medline), 40(5), pp.
619 S40–S46. doi: 10.1097/INF.0000000000002773.
620 https://journals.plos.org/plosone/article?id=10.1371/journal.pone.0102329

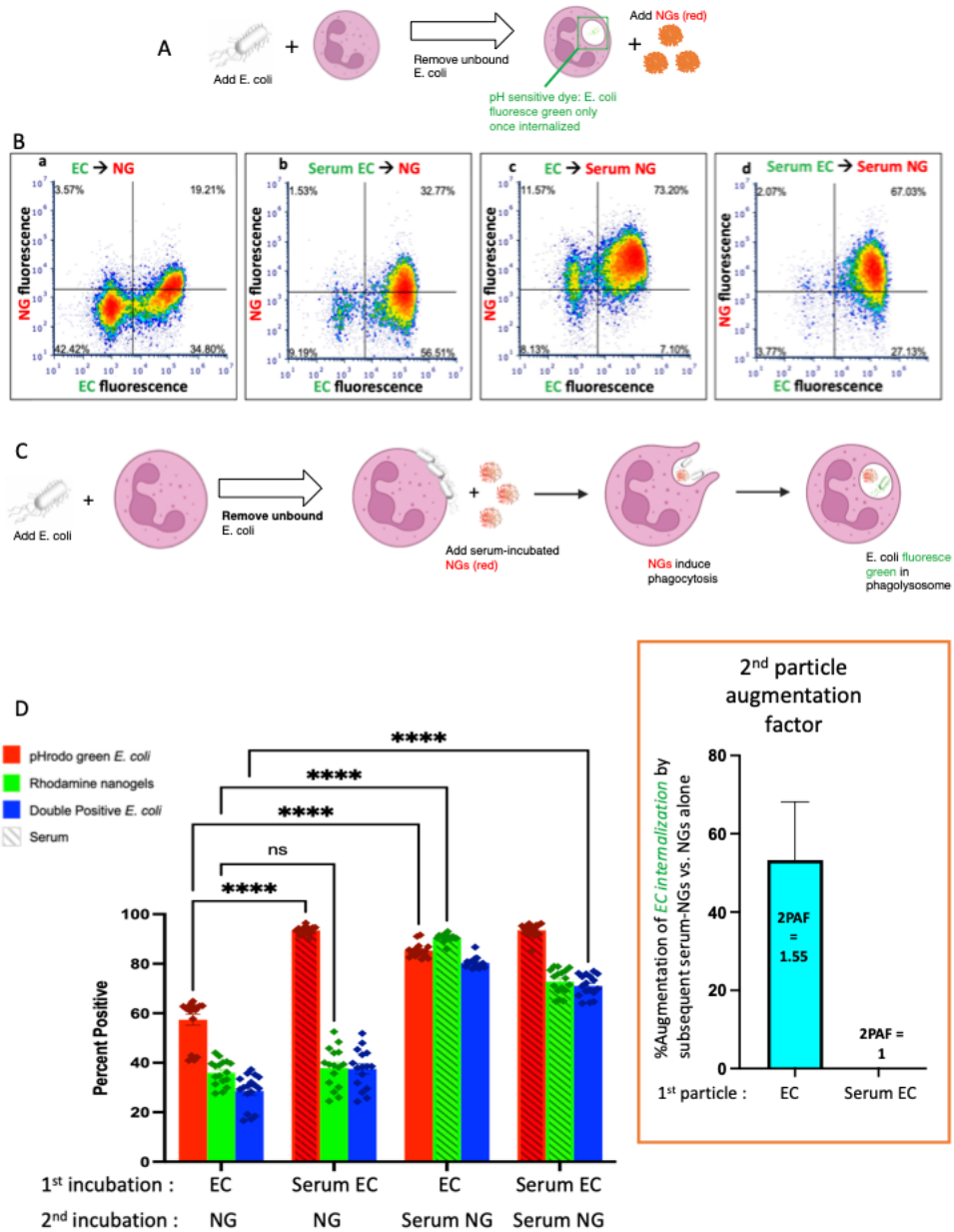

Figure 1. Nanogels augment phagocytosis of *E. coli*. A) Neutrophils were incubated with pH-sensitive fluorescent *E. coli* that only fluoresce in the low pH of the phagosome, thus allowing detection of their phagocytosis. Notably, *E. coli* that bind to the exterior of neutrophils but are not internalized do *not* fluoresce. First neutrophils were exposed to green *E. coli*, thoroughly washed to remove unbound *E. coli*, and then incubated with red nanogels ("NG"). Importantly, before exposure to the neutrophils, select aliquots of nanogels and *E. coli* were opsonized by serum and thoroughly washed before exposure to neutrophils. B) Representative dot-plots of the neutrophils subjected to flow cytometry *after* the second incubation, examining for green fluorescence (x-axis, indicating phagocytosis of the *E. coli*) and red (y-axis, nanogels). At the top of each subpanel, we indicate whether the *E. coli* (EC) were not exposed to serum (simply "EC") or were serum-opsonized ("Serum EC"); similar notation is used for nanogels without serum exposure (simply "NG") or those that were serum-opsonized ("Serum NG"). Neutrophils positive for uptake of green *E. coli* are represented as dots to the right of the vertical bar in the middle of the plot, with that

635 threshold determined by measuring fluorescence of *E. coli* not exposed to any *E. coli*. Similarly,
636 neutrophils represented as dots above the horizontal line are positive for red nanogels C)
637 Diagram of the proposed mechanism underlying this 2PFE of 1.5. Some *E. coli* remain bound to
638 the neutrophil surface even after thoroughly washing the cells (second neutrophil image), but
639 these surface-bound *E. coli* do not fluoresce since buffer pH of ~7 prevents their pH-sensitive dye
640 from fluorescing. When these neutrophils encounter Serum NG, they phagocytose not just the
641 nanogels, but also the *E. coli* (third neutrophil image), causing the *E. coli* to fluoresce in the low
642 pH of the phagosome (fourth neutrophil). D) Quantification of the flow cytometry experiments with
643 n=6 biological replicates for each sample. The bottom axis lists for the 1st and 2nd incubations
644 whether the *E. coli* and nanogels were first exposed to serum or not. The y-axis lists the % of
645 neutrophils that were positive for phagocytosed *E. coli* (recalling that pH-sensitive E.coli on the
646 *surface* of neutrophils will *not* fluoresce). Among the many bars to compare, the most important
647 is comparing the first vs third red bars, which both measure the % of neutrophils that
648 phagocytosed non-serum-opsonized *E. coli* (EC). When the second incubation was with NG (not
649 serum exposed), only 55% of neutrophils were positive for the EC presented during the first
650 incubation. However, when the second incubation was with *Serum* NG, 85% of neutrophils were
651 positive for the EC presented during the first incubation. This important ratio (first vs third red
652 bar), which we call the "2nd particle augmentation factor (2PAF)" was ~1.55 (*inset in box*, red),
653 and *measures the fold-increase in phagocytosis of ECs induced by Serum NG (compared to non-*
654 *serum-exposed NG, which serves as an internal control)*. Notably, while Serum NG augment
655 uptake of (non-opsonized) EC by 50% (2PAF of 1.5), Serum NG do not significantly augment
656 neutrophil uptake of Serum EC (second vs fourth red bar, 2PAF = 1.0, blue bar in inset). Thus,
657 Serum NG only augment phagocytosis of non-opsonized *E. coli*.

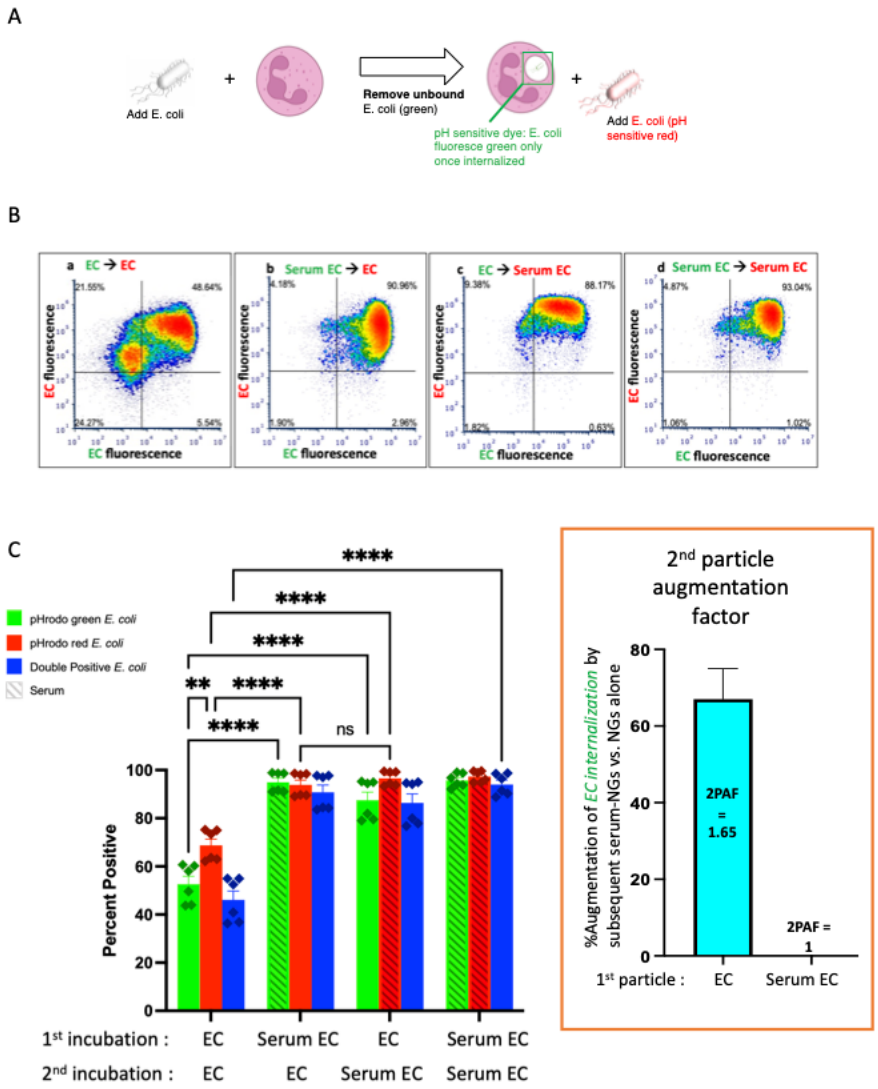

Figure 2. Similarly to serum-opsonized nanogels, serum-opsonized *E. coli* augment internalization of non-opsonized *E. coli*. A) Experimental scheme, similar to Figure 1A, but the second incubation was with *E. coli*. Note the first incubation was green E.coli, while the second was red *E. coli*. This experiment tests if, similar to serum-opsonized nanogels, *E. coli* can augment phagocytosis of previously delivered *E. coli*. B) Representative dot-plots of the neutrophils, using the same notation as Fig 1. C) Quantification of flow cytometry experiments (n=6 biological replicates). Analogous to Fig 1, the most important comparison is the first vs third green bars, which both measure the % of neutrophils that phagocytosed non-serum-opsonized green *E. coli* (EC) which were present during the first incubation. When the second incubation was also with EC, only 50% of neutrophils were positive for the green EC presented during the first incubation. However, when the second incubation was with Serum EC, 85% of neutrophils were positive for the green EC presented during the first incubation. Thus, when the first particle is EC, the "2nd particle augmentation factor (2PAF)" was ~1.65 (inset, red). While Serum EC augment uptake of (non-opsonized) EC by 65%, Serum EC do not significantly augment phagocytosis of Serum EC that were present in the first incubation (2PAF = 1.0, blue bar in inset). Also notable is that Serum EC delivered as the first particle augments the uptake of EC delivered second

675 (second red bar vs first red bar), showing the 2PAF effect does not depend on other order in which
676 particles are delivered.

677

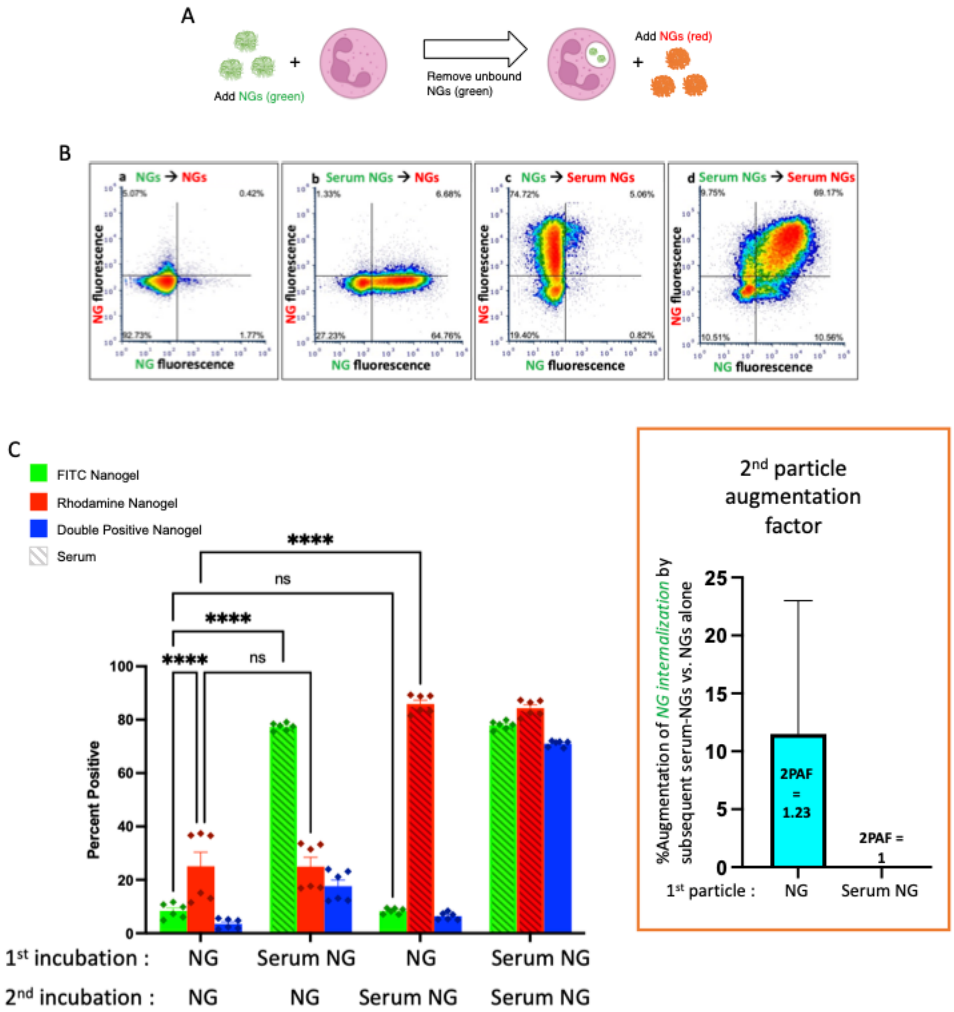

Figure 3. Serum-opsonized nanogels do not augment neutrophil association with previously delivered nanogels. A) Similar to the paradigm described in Figure 1, neutrophils were exposed to green nanogels, followed by washing to remove unbound neutrophils, then exposed to red nanogels, washed, and then the neutrophils were subjected to flow cytometry. B) Representative flow cytometry dot-plots. C) Quantification of n=6 biological replicates. The most notable comparison is the first and third green bars, which indicate that serum-opsonized nanogels ("Serum NGs") do not augment the fraction of neutrophils that are positive for binding to non-serum-exposed nanogels ("NGs"). Notably, unlike the pH-sensitive *E. coli* used in Figs 1 & 2, nanogels fluoresce both when bound to the neutrophil surface and when in the phagosome. Thus, it is possible that some NGs are bound to the neutrophil surface and then internalized after exposure to Serum NGs, but this assay cannot detect such internalization events. Another major result of this set of conditions is that Serum NGs have uniformly high uptake into neutrophils regardless of whether the neutrophils were first exposed to other nanogels (NGs or Serum NGs), suggesting the neutrophils do not saturate their uptake of Serum NGs in this dynamic range (they do not "get full").

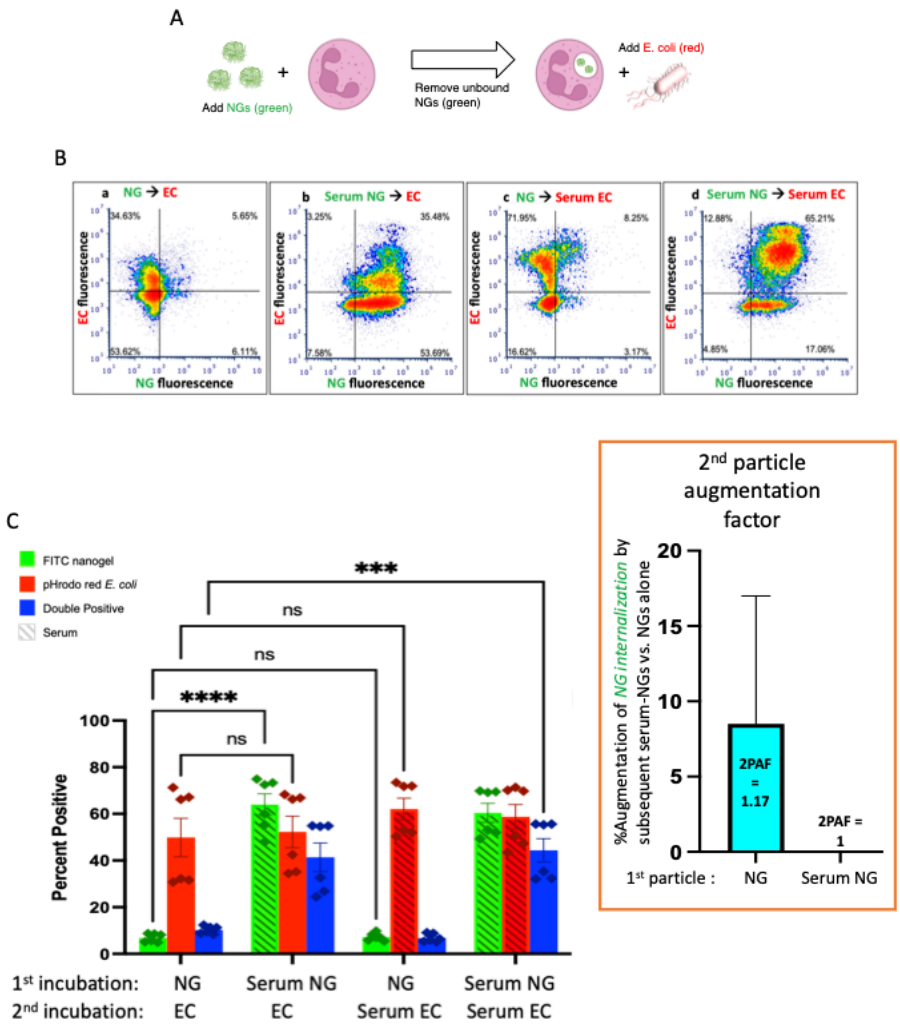

Figure 4. Serum-opsonized *E. coli* are also unable to augment neutrophil association with previously delivered nanogels. A) Here the first particle is nanogels, while the second particle is *E. coli*. Thus, this tests if EC can augment neutrophil association with nanogels. B) Representative flow cytometry dot-plots. C) Quantification of n=6 biological replicate. The most notable comparison again is the first and third green bars, which indicate that serum-opsonized *E. coli* ("Serum ECs") do not augment the fraction of neutrophils that are positive for binding to non-serum-exposed nanogels ("NGs"). A second important result is that nanogels do *not* decrease neutrophil phagocytosis of *E. coli* (all red bars are equal). This is clinically relevant because it means that if a neutrophil phagocytoses a nanogel and then later encounters a bacterium, the nanogel will not reduce the likelihood of uptake of the bacterium. Thus, the nanogels do not induce immunosuppression by this metric.

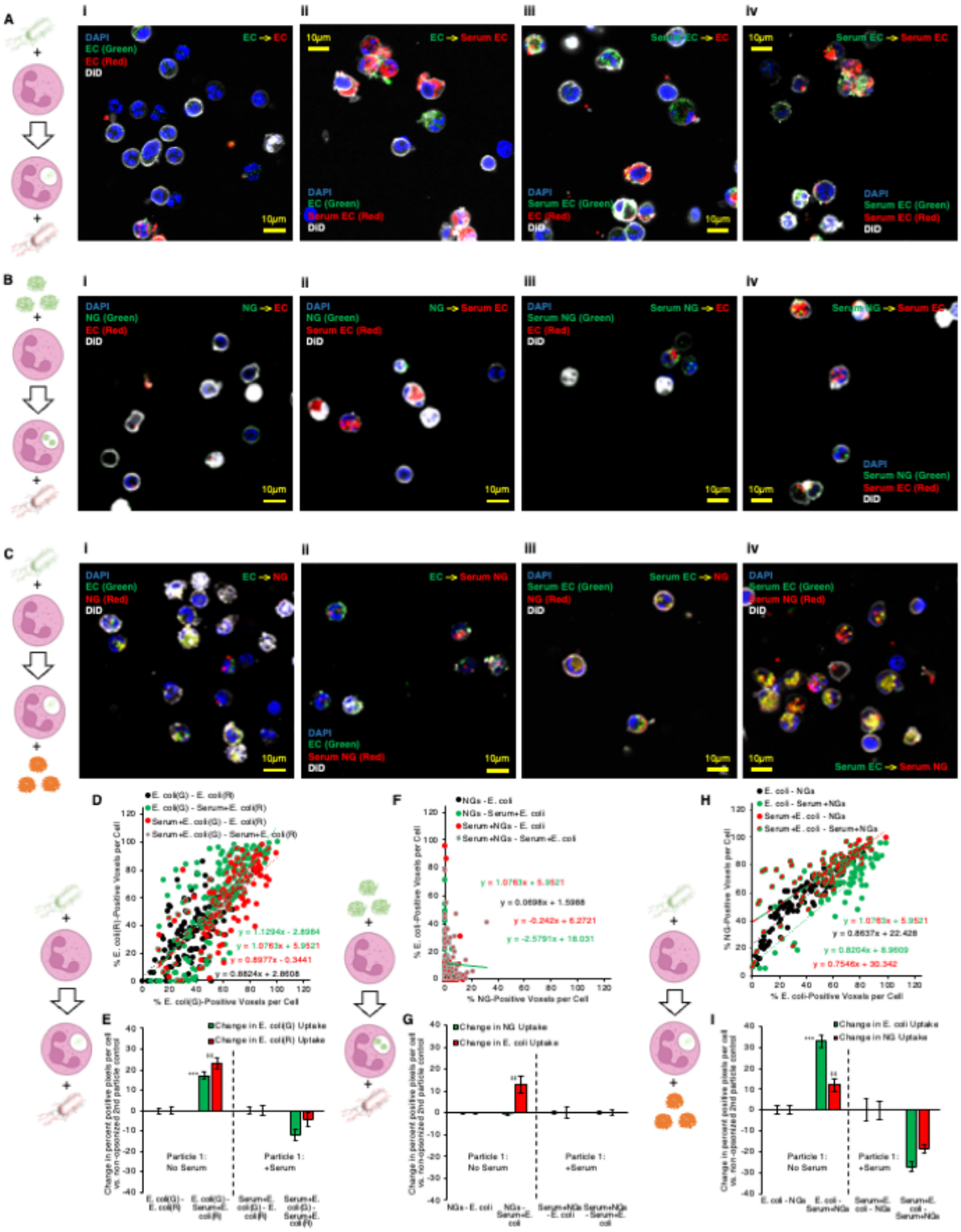

Figure 5. Microscopy confirms that serum-opsonized nanogels improve internalization of non-opsonized *E. coli*, and that they then share significant colocalization within

neutrophils. A) Example images of neutrophils given two different labeled *E. coli* doses in sequence, for different serum pretreatment conditions applied to the *E. coli*. B) Example images of neutrophils given lysozyme-dextran nanogels (NGs) prior to *E. coli*, for different serum pretreatment conditions applied to the NGs and *E. coli*. C) Example images of neutrophils given *E. coli* prior to NGs, for different serum pretreatment conditions applied to the NGs and *E. coli*. Each point depicted in (D) indicates data for one cell, in imaging experiments as in (A). The horizontal coordinate indicates quantity of green *E. coli* signal and the vertical coordinate indicates quantity of red *E. coli* signal. Higher slope indicates that cells generally have more red *E. coli*, relative to quantity of green *E. coli*. All conditions showed strong positive correlation between red and green signal, indicating that cells taking up green *E. coli*, given first, were likely to take up red *E. coli*, given subsequently. E) 2PAF enhancement of first particle (green) *E. coli* by addition of serum to second particle (red) *E. coli*., in imaging experiments as in (A). Bars 3-4 and 7-8 in (E) show the per-cell average difference in uptake of each color *E. coli* induced by serum treatment of second particle (red) *E. coli*. Green bars >0 indicate serum treatment of second particle (red) *E. coli* increases the average per cell uptake of first particle (green) *E. coli*. F-G) Data is as presented in (D-E), but for imaging experiments as in (B), wherein NGs were given to neutrophils before *E. coli*. There was poor correlation between per-cell NG signal and *E. coli* signal, for all serum pretreatment conditions, indicating that neutrophil uptake of NGs does not predict subsequent uptake of *E. coli*. G) indicates no 2PAF effect exerted by second particle *E. coli* on NGs. H-I) Data is as presented in (D-E) and (F-G), but for imaging experiments as in (C), wherein *E. coli* was given to neutrophils before NGs. In (H), there was strong correlation between NG and *E. coli* uptake in any given cell, when *E. coli* was taken up before neutrophil exposure to NGs. In (I), bar 3 indicates that opsonized second particle NGs enhance uptake of non-opsonized first particle *E. coli*.